JACS
JOURNAL OF THE AMERICAN CHEMICAL SOCIETY
Communication
pubs.acs.org/JACS

Synergistic Role of Dopants on the Morphology of Alloyed Copper Chalcogenide Nanocrystals

Ajay Singh,[†,‡] Amita Singh,[†,‡] Jim Ciston,[§] Karen Bustillo,[§] Dennis Nordlund,[∥] and Delia J. Milliron*[,†]

[†]McKetta Department of Chemical Engineering, The University of Texas at Austin, Austin, Texas 78712, United States
[‡]The Molecular Foundry and [§]National Center for Electron Microscopy, Lawrence Berkeley National Laboratory, Berkeley, California 94720, United States
[∥]Stanford Synchrotron Radiation Lightsource, Stanford, California 94309, United States

Supporting Information

ABSTRACT: The presence of antimony, as a dopant in the colloidal growth reaction for $CuIn_{1-x}Ga_xS_2$ (CIGS) nanocrystals, causes end-to-end fusion of nanorod pairs into nanodumbbells at high yield. The influence of the dopant on shape is indirect; antimony catalyzes the incorporation of gallium, which is found in high concentration at the junction between the fused nanorods.

Solution routes to semiconductor inorganic nanocrystals (NCs) have made dramatic advancements in the last two decades.[1] Specifically, synthesis schemes have evolved from simple binary (two-element) semiconductors to more complex compound (few-element) semiconductor NCs, which have now been routinely achieved with excellent control of their size, shape, and crystal structure.[1c,2] The ability to control these properties at the nanoscale has allowed correlations to be made between NC structure and their optical, magnetic, and electronic properties, which has implicated these materials in various applications ranging from biomarkers to photovoltaics.[1,2] Another way to tune such properties while keeping the NC morphology (size, shape, and crystal structure) constant is by alloying or doping, incorporating other atoms or ions into host lattices to yield more complex hybrid materials ranging from ternary to multicomponent systems.[1c,2,3] However, recent studies showed that the incorporation of dopants into the host lattices not only altered the composition of the NCs but also modified NC nucleation and growth rates, ultimately impacting NC morphology. Here, we report a striking example where two dopants act synergistically to cause the dimerization of multinary nanorods (NRs) into nanodumbbells (NDBs).

Recently, multicomponent copper chalcogenide-based compound semiconductor NCs ($CuIn_{1-x}Ga_xS_2$ (CIGS), $CuInS_2$ (CIS), Cu_2SnSe_3 (CTSe), Cu−In−Zn−S (CIZS), $Cu_2CdZnSnS_4$ (CCdZTS), Cu_2ZnSnS_4 (CZTS), etc.) are attracting considerable attention due to the ability to compositionally tailor their (direct) optical band gaps over a wide range, their high absorption coefficients, and because they contain elements with lower toxicity than their cadmium- and lead-based analogues.[4] These materials have already shown great potential in low-cost photovoltaics, thermoelectrics, and for photocatalysis.[2b,c,4,5] Controlling the shape of NCs enables new possibilities for assembly and device integration, motivating the synthesis of anisotropic morphologies.[2a,d−g] Yet, despite recent progress in colloidal synthesis, it has been challenging to prepare shape-controlled, anisotropic compound semiconductor NCs.[4a,b,5a−d] Conventionally, shape control of NCs involves deliberate selection of long chain aliphatic organic surfactants with amines, thiols, and carboxylic and phosphonic acid functional groups that selectively bind to different crystal facets.[1c,2] Dopants (that become incorporated in the NCs) and foreign atoms/ions (not incorporated) have also been shown to stabilize or direct specific crystallographic phases and morphologies of NCs.[3a,6] One example of a dopant influencing NC morphology is the dramatic impact of magnesium on the shape of ZnO NCs, changing from tetrapods to ultrathin nanowires.[6a] Furthermore, the presence of foreign aluminum ions in the reaction solution enables the formation of copper selenide nanocubes by manipulating the nucleation and the kinetics of growth in different crystallographic directions.[6b] There are numerous other examples in the literature of the use of dopants and foreign ions to control the shape of metal (Au, Pt, PtNi, etc.), metal oxide (ZnO, TiO_2, ITO, etc.), and up-conversion ($NaYF_4$, Y_2O_3, etc.) NCs.[6] However, no such studies have reported the influence of dopants on the morphology of copper based compound semiconductor chalcogenides, perhaps owing to their complex compositions; we see here that this complexity allows for unusual cooperative influence of multiple dopants in combination.

Here, we present the direct observation of a morphological transformation under the synergistic influence of antimony and gallium dopants on copper indium disulfide (CIS) NCs. Antimony was targeted as an interesting dopant since it was previously found to promote crystal growth during sintering or selenization in thin films or nanocrystals of multicomponent copper chalcogenide semiconductors (CIGS and CZTS).[2c,4i] We found that the presence of antimony catalyzes the incorporation of gallium at an earlier stage in the growth process and that together these dopants cooperatively induce the head-to-head coupling of NRs to form dimers in the shape of NDBs. NDBs do not form in the presence of gallium or antimony alone (only individual copper indium gallium sulfide (CIGS) or Sb-doped CIS NRs are formed).

CIS NRs were prepared using a hot injection colloidal synthesis route adapted from previously published methods.[5a,b]

Received: March 19, 2015
Published: May 14, 2015

DOI: 10.1021/jacs.5b02880
J. Am. Chem. Soc. 2015, 137, 6464−6467

To dope CIS NRs with trivalent gallium and antimony, acetylacetonate and acetate precursors, $Ga(acac)_3$ and $Sb(ac)_3$, were introduced while keeping all other parameters unchanged. While gallium doping alone yields CIGS NRs, codoping with gallium and antimony results in a high-yield of NDBs that are approximately twice as long as the CIGS NRs and are thinner in diameter at their midpoint (annular dark-field scanning transmission electron microscopy, ADF-STEM; Figure 1a,b). By

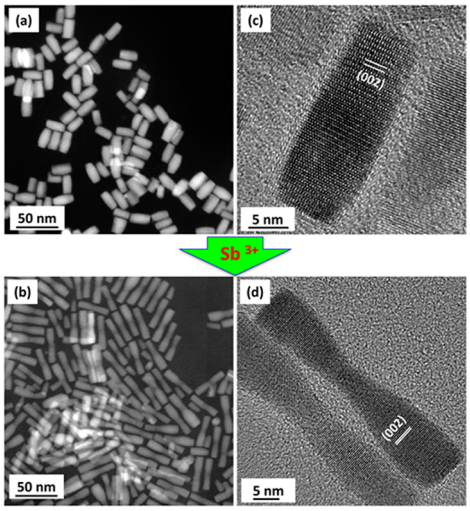

Figure 1. (a, b) Annular dark-field STEM (ADF-STEM) images of CIGS NRs and Sb-doped CIGS NDBs and corresponding HRTEM images (c,d).

high-resolution transmission electron microscopy (HRTEM; Figure 1c) the CIGS NRs are found to be defect-free single crystals as evidenced by the continuous lattice fringes with *d*-spacing of 3.18 Å, corresponding to (002) lattice planes of the hexagonal structure of CIGS.[5a] The NDBs formed by adding $Sb(ac)_3$ to the NC reaction solution are also highly crystalline by HRTEM with similar *d*-spacing of the lattice planes perpendicular to their long axis (Figures 1d and S1 in the Supporting Information, SI).

To assess the role of Sb^{3+} in forming NDBs, we systematically tuned the amount of Sb^{3+} ion added while maintaining a fixed concentration of Ga^{3+} and all other precursors for the NCs. Increasing the molar ratio (Sb/In + Ga + Sb) progressively transforms the NCs from NRs to NDBs (TEM, Figure 2a–c). NDBs begin to form at a minimum Sb ratio of around 3% (Figure 2b). As the dopant concentration is increased further, most of the NCs obtained are NDB-shaped with only a few NRs present, which are around half the length of the NDBs. These NRs and NDBs were further characterized by powder X-ray diffraction (XRD; Figure 2d). The XRD patterns of CIGS NCs with varying Sb concentrations consist of a single set of 2θ peaks corresponding to the hexagonal wurtzite structure, indicating that the presence of Sb^{3+} in the CIGS NCs does not substantially modify the crystal structure. However, as XRD is not sufficient to completely rule out the presence of binary and ternary impurities that may have overlapping diffraction patterns, we further characterized the materials with Raman spectroscopy. At all Sb doping levels, the Raman spectra are similar, showing an intense peak at 291 cm^{-1} corresponding to the main A_1 mode and a broad peak around 343 cm^{-1} due to the $B_2^{(3)}(L)$ and $E^{(6)}(L)$ modes (Figure 2e).[7] The absence of other peaks related to possible impurities (Cu_2S, Cu_2SbS_3, Cu–Au type ordering, etc.)

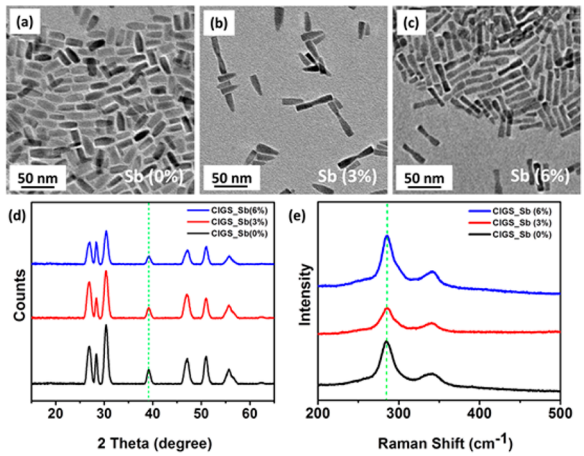

Figure 2. (a–c) TEM images of CIGS NCs (R1, 30 min growth time) obtained at various molar fraction of dopant present in the reaction flask and (d) their respective XRD and (e) Raman analysis.

is clear evidence of the single-phase nature of the CIGS and Sb-doped CIGS NCs.

Aliquot studies were performed to investigate the process of NDB formation and to determine the evolution of NC composition and morphology during synthesis. In our synthetic method, all the metal precursors are present in the initial reaction mixture, then thiols (1-dodecanethiol (1-DDT) and *tert*-dodecanethiol (*t*-DDT)) are injected to initiate the crystallization reaction. When Sb is present, the NC shape evolves from spherical particles to anisotropic NDBs between 3 and 5 min after injection of thiol (Figure 3a–d). The initial product, formed within 3 min, consists of spherical NCs with a diameter of 6 ± 0.5 nm (Figure 3a). Based on XRD (Figure S2a) and energy dispersive X-ray spectroscopy (EDS) analysis (Figure S3) the spherical NCs are mixed phases of copper sulfide. Thus, consistent with previously published reports on CIGS, CTSe, and CIZS NCs,[5b–d,8a] our compound semiconductor synthesis occurs by the initial formation of binary materials and subsequent incorporation of other metal ions.[5b–d] At longer reaction times, elongated morphologies (short NRs, Figure 3b) are found, and the crystal structure is a hexagonal phase (XRD, Figure S2b) matched to the wurtzite structure of $CuInS_2$ (CIS) with no indication yet of gallium incorporation (EDS, Figure S3). The hexagonal phase for these materials is metastable in bulk and has recently been found in colloidal NCs.[3b,c,4a,b,5a–c] As growth proceeds, in the presence of both Ga and Sb, NDBs are formed (Figure 3c,d) and Ga is incorporated (EDS, Figure S3c,d). At the same time, the XRD peaks shift to higher 2θ, indicating a lattice contraction (Figure S2). It is difficult to analyze Sb incorporation by EDS mapping since the Sb and In L-edge peaks overlap and the Sb K-edge peak is too weak to produce a meaningful map, so X-ray photoelectron spectroscopy (XPS) and inductively coupled plasma atomic emission spectroscopy (ICP-AES, Table S1) were used to investigate the Sb concentration in NDBs. All the elements (Cu, In, Ga, Sb, and S) are found to be present in the oxidation states expected for substitutional mixing of Ga and Sb on the In sublattice of CIS (Figure S4 and further discussion in SI).

To this point, the exact role of Sb^{3+} ions in NDB formation is not clear, but elemental mapping by EDS gives new insight (Figure 3e). Although the spatial distribution of Sb cannot be resolved in detail, averaging over many pixels allowed us to uncover an enrichment of Sb in the neck region (Figure S8).

DOI: 10.1021/jacs.5b02880
J. Am. Chem. Soc. 2015, 137, 6464–6467

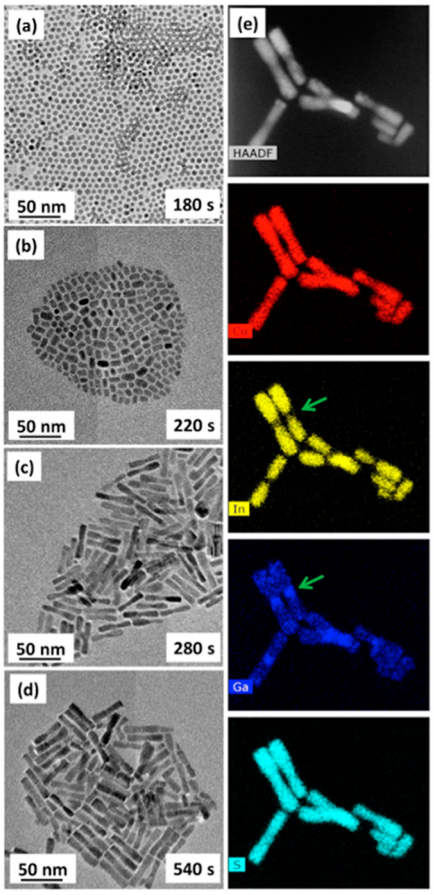

Figure 3. (a–d) TEM images of the NCs obtained at successively higher reaction times during CIGS NDBs synthesis (Sb = 6%). (e) ADF-STEM image and STEM-EDS elemental mapping of NDBs.

Furthermore, there is a striking feature seen in the gallium and indium maps. Evidently, the very center of each dumbbell is gallium rich and indium poor (e.g., green arrows, additional detail in SI). Together with the concurrent appearance of NDBs and lattice-incorporated Ga, this spatial distribution suggests that Ga incorporation is necessary for the formation of NDBs. To validate this hypothesis, we purposely synthesized Sb-doped CIS NCs with no gallium in the reaction. Interestingly, no NDBs were obtained but only NRs were formed (Figure 4). XPS

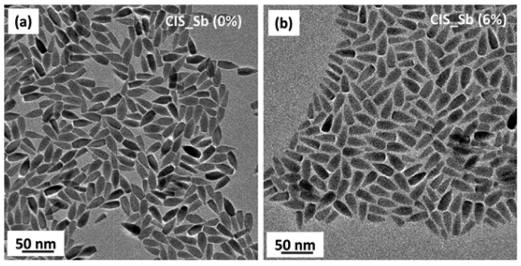

Figure 4. TEM of (a) undoped and (b) Sb-doped CIS NRs.

analysis confirms that Sb is incorporated in the CIS NRs (Figure S5), so we conclude that Sb doping is not *directly* responsible for inducing NDB formation. Rather, it seems that Sb catalyzes the incorporation of Ga, which ultimately drives NRs to dimerize as NDBs.

Not only do synergistic interactions between Ga and Sb change the NC morphology, they substantially modify the kinetics of NC growth. For instance, with Ga present and Sb absent, the initial stage of crystallization is delayed so that copper sulfide NCs appear after 5 min, while they are already formed at 3 min when Ga *and* Sb are present (further discussion in SI, Figure S6). Another striking difference in reaction kinetics is the reaction time until Ga becomes incorporated into the CIS NRs. In our Sb-free CIGS synthesis, similar to the results of Ryan and co-workers,[5b] Ga incorporation was found 10 min or more after injection of the thiol. But in the presence of Sb, Ga incorporation starts already during the first 5 min, which suggests that Sb^{3+} catalyzes the reactivity of gallium monomers toward precipitation at the NC surface. This impact of Sb on the reactivity of the gallium precursor may prove useful for synthesis of CIGS NCs. In previous studies of CIGS NCs, gallium incorporation into CIS required long reaction time or high temperature to initiate the ion exchange process (rationalized by the hard Lewis acidity of Ga^{3+} compared to In^{3+}).[5b] The resulting long reaction time required to reach the target composition can have deleterious effects on the NCs (e.g., broader size distribution, defects, and secondary growth).[5b] Hence, the cooperative doping effect we observed may be a powerful new strategy for tuning NC composition.

From the experimental results obtained, we hypothesize that the growth mechanism for NDBs follows the discrete steps depicted in Figure 5. The reaction begins with the formation of

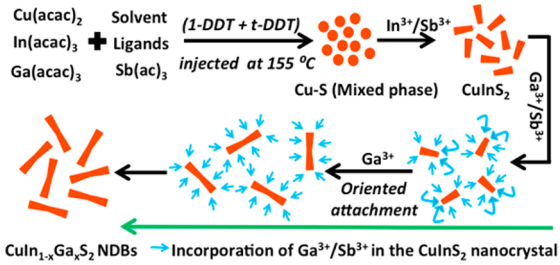

Figure 5. Schematic representation of the growth mechanism leading to NDB formation.

binary NCs (copper sulfide), which then evolve to ternary CIS NRs. At this point, catalyzed by the presence of Sb^{3+}, gallium starts incorporating into the growing CIS NRs. Then, apparently, these NRs coupled to each other at their gallium-rich ends by an oriented attachment mechanism. These NDBs incorporate additional gallium as they grow larger in diameter in the final stage of growth (Figure 3d). It is possible that a related synergistic mechanism, rather than any direct effect, underlies the observation that Sb^{3+} promotes sintering in multicomponent copper-based photovoltaic thin films.[2c,4i] Further evidence for NR coupling to form NDBs was found by HRTEM and HAADF-STEM analysis (Figure 6). Defects (stacking faults in Figure 6b or dislocations in Figure 6e) present in the thin sections of the NDBs support the mechanism of oriented attachment. Indeed, similar head-to-head coupling of nanorods of metal chalcogenides (CIZS, ZnSe, CdS) has been previously reported.[8a−d]

In summary, we describe the cooperative effect of trivalent dopants, gallium and antimony, on the shape of complex compound chalcogenide (CIS-based) NCs. One dopant (Sb) catalyzes the incorporation of the other (Ga), tuning the reaction kinetics and leading to the formation of Sb-doped CIGS NDBs.

DOI: 10.1021/jacs.5b02880
J. Am. Chem. Soc. 2015, 137, 6464−6467

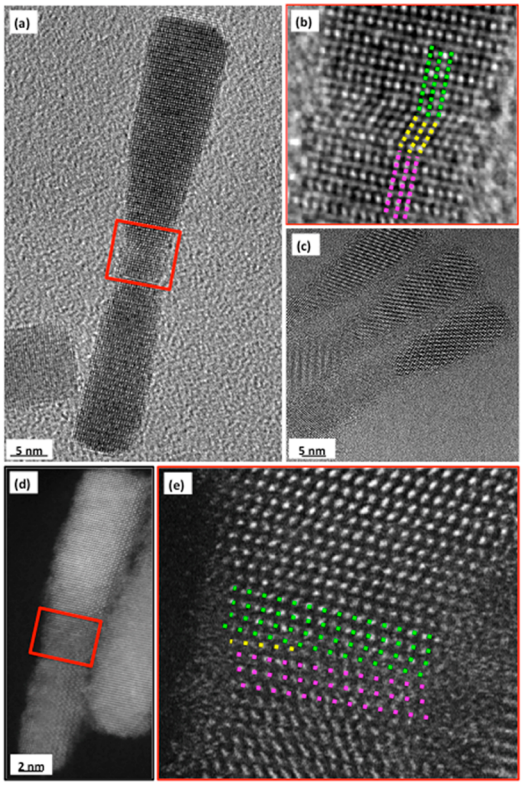

Figure 6. (a–c) HRTEM and (d,e) HAADF-STEM images of NDBs. In panel e, green and purple dots represent atomic planes on each side of the crystal defect region (yellow dots).

■ ASSOCIATED CONTENT

Supporting Information

Full synthetic details, additional HRTEM images of NDBs and XPS, ICP-AES, and EDS analysis. The Supporting Information is available free of charge on the ACS Publications website at DOI: 10.1021/jacs.5b02880.

■ AUTHOR INFORMATION

Corresponding Author

*milliron@che.utexas.edu

Notes

The authors declare no competing financial interest.

■ ACKNOWLEDGMENTS

This work was performed in part at the Molecular Foundry, Lawrence Berkeley National Laboratory, a user facility supported by the Office of Science, Office of Basic Energy Sciences, of the U.S. Department of Energy (DOE) under Contract No. DE-AC02-05CH11231. Aj.S. was supported by the Bay Area Photovoltaics Consortium, sponsored by DOE EERE, while Am.S. and D.J.M. were supported by a DOE Early Career Research Program grant to D.J.M. Use of the SSRL, SLAC National Accelerator Laboratory, is supported by DOE under Contract No. DE-AC02-76SF00515. Additional support from the Welch Foundation is gratefully acknowledged (F-1848).

■ REFERENCES

(1) (a) Alivisatos, A. P. *Science* **1996**, *271*, 933. (b) Murray, C. B.; Kagan, C. R.; Bawendi, M. G. *Annu. Rev. Mater. Sci.* **2000**, *30*, 545. (c) Talapin, D. V.; Lee, J. S.; Kovalenko, M. V.; Shevchenko, E. V. *Chem. Rev.* **2010**, *110*, 389.

(2) (a) Krahne, R.; Morello, G.; Figuerola, A.; George, C.; Deka, S.; Manna, L. *Phys. Rep.* **2011**, *501*, 75. (b) Aldakov, D.; Lefrancois, A.; Reiss, P. *J. Mater. Chem. C* **2013**, *1*, 3756. (c) Yuan, M.; Mitzi, D.; Liu, W.; Kellock, A.; Chey, S.; Deline, V. *Chem. Mater.* **2010**, *22*, 285. (d) Rivest, J. B.; Swisher, S. L.; Fong, L.-K.; Zheng, H.; Alivisatos, A. P. *ACS Nano* **2011**, *5*, 3811. (e) Singh, A.; English, N. J.; Ryan, K. M. *J. Phys. Chem. B* **2013**, *117*, 1608. (f) O'Sullivan, C.; Crilly, S.; Laffir, F. R.; Singh, A.; Magner, E.; Ryan, K. M. *Chem. Commun.* **2011**, *47*, 2655. (g) Singh, S.; Singh, A.; Palaniappan, K.; Ryan, K. M. *Chem. Commun.* **2013**, *49*, 10293.

(3) (a) Buonsanti, R.; Milliron, D. J. *Chem. Mater.* **2013**, *25*, 1305. (b) Shen, S.; Wang, Q. *Chem. Mater.* **2013**, *25*, 1166. (c) Regulacio, M. D.; Han, M. Y. *Acc. Chem. Res.* **2010**, *43*, 621.

(4) (a) Singh, A.; Geaney, H.; Laffir, F.; Ryan, K. M. *J. Am. Chem. Soc.* **2012**, *134*, 2910. (b) Wang, Y.-H. A.; Zhang, X.; Bao, N.; Lin, B.; Gupta, A. *J. Am. Chem. Soc.* **2011**, *133*, 11072. (c) Ibáñez, M.; Cadavid, D.; Zamani, R.; García-Castelló, N.; Izquierdo-Roca, V.; Li, W.; Fairbrother, A.; Prades, J. D.; Shavel, A.; Arbiol, J.; Perez-Rodriguez, A.; Morante, J. R.; Cabot, A. *Chem. Mater.* **2012**, *24*, 562. (d) Steinhagen, C.; Panthani, M. G.; Akhavan, V.; Goodfellow, B.; Koo, B.; Korgel, B. A. *J. Am. Chem. Soc.* **2009**, *131*, 12554. (e) Singh, A.; Singh, S.; Levcenko, S.; Unold, T.; Laffir, F.; Ryan, K. M. *Angew. Chem., Int. Ed.* **2013**, *52*, 9120. (f) Yang, C.; Zhou, B.; Miao, S.; Yang, C.; Cai, B.; Zhang, W.-H.; Xu, X. *J. Am. Chem. Soc.* **2013**, *135*, 5958. (g) Wang, J.; Singh, A.; Liu, P.; Singh, S.; Coughlan, C.; Guo, Y.; Ryan, K. M. *J. Am. Chem. Soc.* **2013**, *135*, 7835. (h) Shavel, A.; Arbiol, J.; Cabot, A. *J. Am. Chem. Soc.* **2010**, *132*, 4514. (i) Carrete, A.; Shavel, A.; Fontané, X.; Montserrat, J.; Fan, J.; Ibáñez, M.; Saucedo, E.; Pérez-Rodríguez, A.; Cabot, A. *J. Am. Chem. Soc.* **2013**, *135*, 15982.

(5) (a) Singh, A.; Coughlan, C.; Laffir, F.; Ryan, K. M. *ACS Nano* **2012**, *6*, 6977. (b) Coughlan, C.; Singh, A.; Ryan, K. M. *Chem. Mater.* **2013**, *25*, 653. (c) Wang, J.-j.; Liu, P.; Seaton, C. C.; Ryan, K. M. *J. Am. Chem. Soc.* **2014**, *136*, 7954. (d) Kolny-Olesiak, J.; Weller, H. *ACS Appl. Mater. Interfaces* **2013**, *5*, 12221. (e) Lesnyak, V.; George, C.; Genovese, A.; Prato, M.; Casu, A.; Ayyappan, S.; Scarpellini, A.; Manna, L. *ACS Nano* **2014**, *8*, 8407. (f) Reifsnyder, D. C.; Ye, X.; Gordon, T. R.; Song, C.; Murray, C. B. *ACS Nano* **2013**, *7*, 4307. (g) Mainz, R.; Singh, A.; Levcenko, S.; Klaus, M.; Genzel, C.; Ryan, K.; Unold, T. *Nat. Commun.* **2014**, *5*, 3133. (h) Ibáñez, M.; Zamani, R.; LaLonde, A.; Cadavid, D.; Li, W.; Shavel, A.; Arbiol, J.; Morante, J. R.; Gorsse, S.; Snyder, G. J.; Cabot, A. *J. Am. Chem. Soc.* **2012**, *134*, 4060.

(6) (a) Yang, Y.; Jin, Y.; He, H.; Wang, Q.; Tu, Y.; Lu, H.; Ye, Z. *J. Am. Chem. Soc.* **2010**, *132*, 13381. (b) Li, W.; Zamani, R.; Ibáñez, M.; Cadavid, D.; Shavel, A.; Morante, J. R.; Arbiol, J.; Cabot, A. *J. Am. Chem. Soc.* **2013**, *135*, 4664. (c) Lim, S. I.; Ojea-Jiménez, I.; Varon, M.; Casals, E.; Arbiol, J.; Puntes, V. *Nano Lett.* **2010**, *10*, 964. (d) Lim, B.; Lu, X.; Jiang, M.; Camargo, P. H. C.; Cho, E. C.; Lee, E. P.; Xia, Y. N. *Nano Lett.* **2008**, *8*, 4043. (e) Zhang, J.; Fang, J. Y. *J. Am. Chem. Soc.* **2009**, *131*, 18543. (f) De Trizio, L.; Schimpf, A. M.; Llordes, A.; Gamelin, D. R.; Simonutti, R.; Milliron, D. J. *Chem. Mater.* **2013**, *25*, 3383. (g) Bose, R.; Manna, G.; Pradhan, N. *J. Phys. Chem. C* **2013**, *117*, 20991. (h) Wang, F.; Han, Y.; Lim, C. S.; Lu, Y. H.; Wang, J.; Xu, J.; Chen, H. Y.; Zhang, C.; Hong, M. H.; Liu, X. G. *Nature* **2010**, *463*, 1061.

(7) Izquierdo-Roca, V.; Shavel, A.; Saucedo, E.; Jaime-Ferrer, S.; Álvarez-García, J.; Cabot, A.; Pérez-Rodríguez, A.; Bermudez, V.; Morante, J. R. *Sol. Energy Mater. Sol. Cells* **2011**, *95* (Supplement 1), S83–S8.

(8) (a) Singh, A.; Coughlan, C.; Milliron, D. J.; Ryan, K. M. *Chem. Mater.* **2015**, *27*, 1517. (b) Jia, G.; Sitt, A.; Hitin, G. B.; Hadar, I.; Bekenstein, Y.; Amit, Y.; Popov, I.; Banin, U. *Nat. Mater.* **2014**, *13*, 301. (c) Bertoni, G.; Grillo, V.; Brescia, R.; Ke, X.; Bals, S.; Catellani, A.; Li, H.; Manna, L. *ACS Nano* **2012**, *6*, 6453. (d) O'Sullivan, C.; Gunning, R. D.; Sanyal, A.; Barrett, C. A.; Geaney, H.; Laffir, F. R.; Ahmed, S.; Ryan, K. M. *J. Am. Chem. Soc.* **2009**, *131*, 12250.

DOI: 10.1021/jacs.5b02880
J. Am. Chem. Soc. 2015, 137, 6464–6467